Cell Reports, Volume *9*

Supplemental Information

Ire1 Has Distinct Catalytic Mechanisms for *HAC1* Splicing and RIDD

Arvin B. Tam, Albert C. Koong, and Maho Niwa

Figure S1

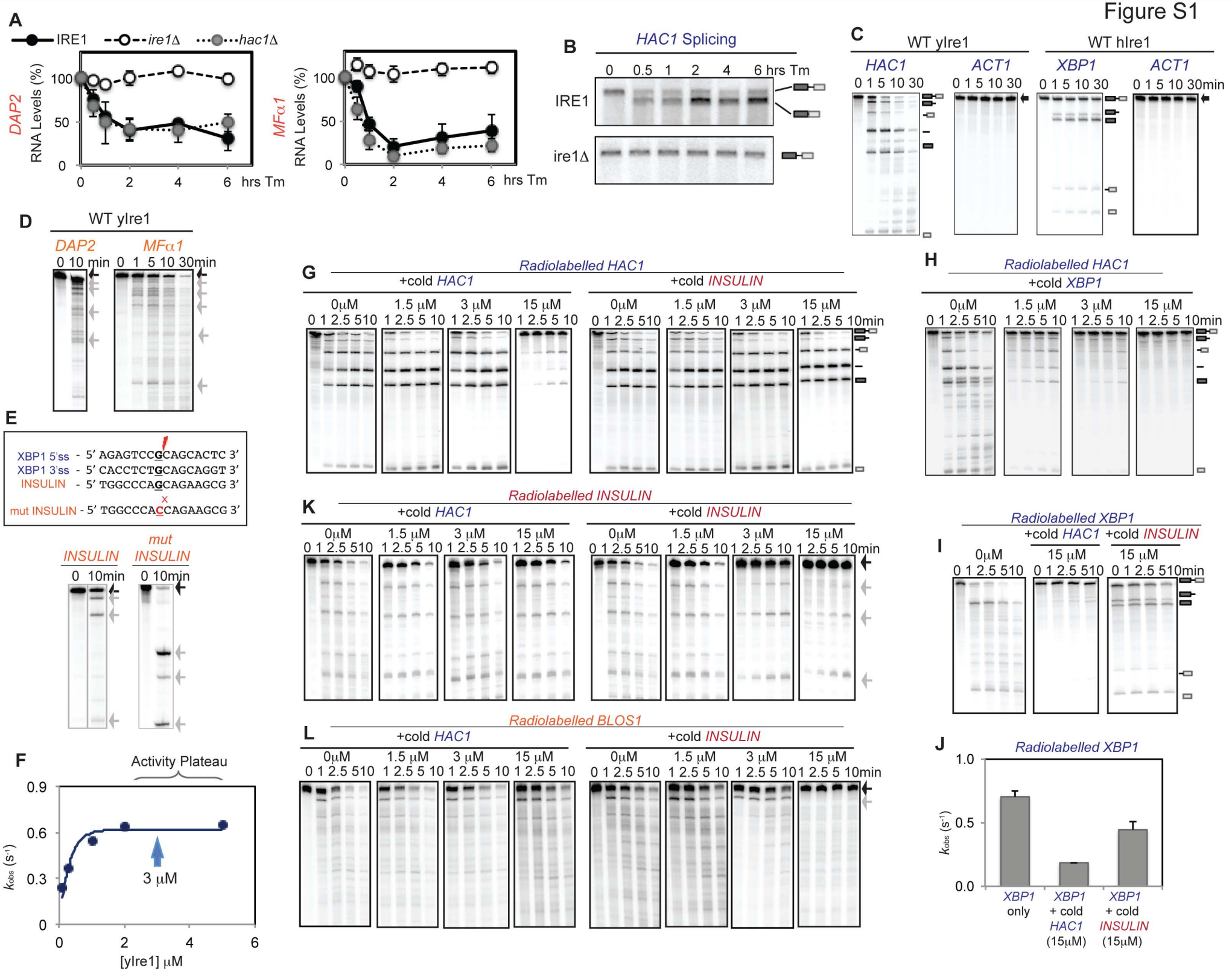
A
IRE1
ire1Δ
hac1Δ
DAP2
RNA Levels (%)
100
50
0
0 2 4 6 hrs Tm
MFα1
RNA Levels (%)
100
50
0
0 2 4 6 hrs Tm
B
HAC1 Splicing
0 0.5 1 2 4 6 hrs Tm
IRE1
ire1Δ
C
WT yIre1
HAC1
0 1 5 10 30
ACT1
0 1 5 10 30
WT hIre1
XBP1
0 1 5 10 30
ACT1
0 1 5 10 30min
D
WT yIre1
DAP2
0 10 min
MFα1
0 1 5 10 30min
E
XBP1 5'ss - 5' AGAGTCCGCAGCACTC 3'
XBP1 3'ss - 5' CACCTCTGCAGCAGGT 3'
INSULIN - 5' TGGCCCAGCAGAAGCG 3'
mut INSULIN - 5' TGGCCCACCAGAAGCG 3'
INSULIN
0 10min
mut INSULIN
0 10min
F
Activity Plateau
0.9
0.6
0.3
0
kobs (s-1)
3 μM
0 2 4 6
[yIre1] μM
G
Radiolabelled HAC1
+cold HAC1
+cold INSULIN
0μM 1.5 μM 3 μM 15 μM
0 1 2.5 5 10 1 2.5 5 10 1 2.5 5 10 1 2.5 5 10
0μM 1.5 μM 3 μM 15 μM
0 1 2.5 5 10 1 2.5 5 10 1 2.5 5 10 1 2.5 5 10min
H
Radiolabelled HAC1
+cold XBP1
0μM 1.5 μM 3 μM 15 μM
0 1 2.5 5 10 1 2.5 5 10 1 2.5 5 10 1 2.5 5 10min
K
Radiolabelled INSULIN
+cold HAC1
+cold INSULIN
0μM 1.5 μM 3 μM 15 μM
0 1 2.5 5 10 1 2.5 5 10 1 2.5 5 10 1 2.5 5 10
0μM 1.5 μM 3 μM 15 μM
0 1 2.5 5 10 1 2.5 5 10 1 2.5 5 10 1 2.5 5 10min
I
Radiolabelled XBP1
+cold HAC1
+cold INSULIN
0μM
15 μM
15 μM
0 1 2.5 5 10
0 1 2.5 5 10
0 1 2.5 5 10min
L
Radiolabelled BLOS1
+cold HAC1
+cold INSULIN
0μM 1.5 μM 3 μM 15 μM
0 1 2.5 5 10 1 2.5 5 10 1 2.5 5 10 1 2.5 5 10
0μM 1.5 μM 3 μM 15 μM
0 1 2.5 5 10 1 2.5 5 10 1 2.5 5 10 1 2.5 5 10min
J
Radiolabelled XBP1
1.0
0.5
0.0
kobs (s-1)
XBP1 only
XBP1 + cold HAC1 (15μM)
XBP1 + cold INSULIN (15μM)

Figure S2

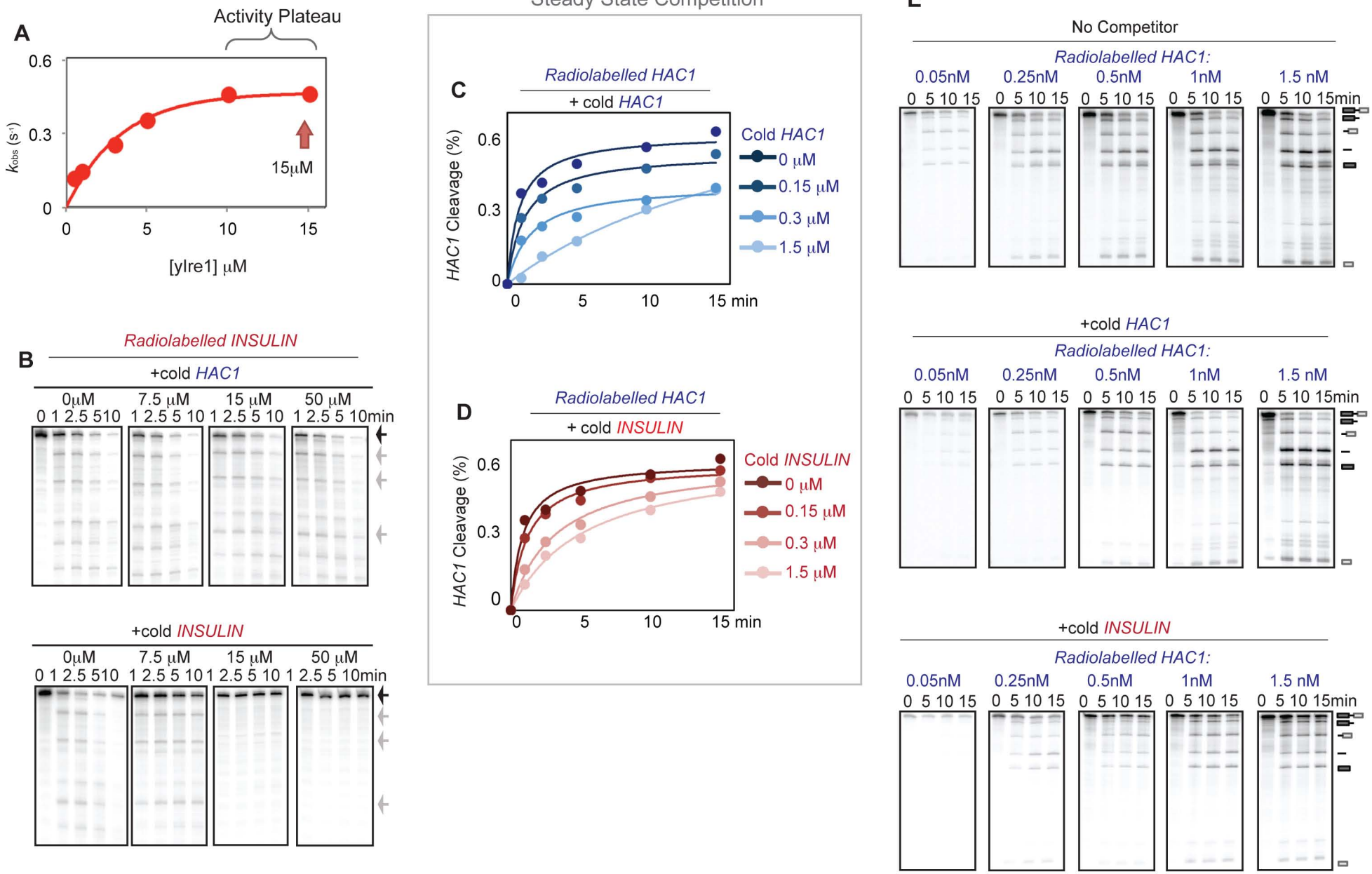
A
Activity Plateau
0.6
0.3
0
k_{obs} (s^{-1})
15μM
0
5
10
15
[ylre1] μM
B
Radiolabelled INSULIN
+cold HAC1
0μM
7.5 μM
15 μM
50 μM
0 1 2.5 5 10
1 2.5 5 10
1 2.5 5 10
1 2.5 5 10min
+cold INSULIN
0μM
7.5 μM
15 μM
50 μM
0 1 2.5 5 10
1 2.5 5 10
1 2.5 5 10
1 2.5 5 10min
Steady State Competition
C
Radiolabelled HAC1
+ cold HAC1
HAC1 Cleavage (%)
0.6
0.3
0
0
5
10
15 min
Cold HAC1
0 μM
0.15 μM
0.3 μM
1.5 μM
D
Radiolabelled HAC1
+ cold INSULIN
HAC1 Cleavage (%)
0.6
0.3
0
0
5
10
15 min
Cold INSULIN
0 μM
0.15 μM
0.3 μM
1.5 μM
E
No Competitor
Radiolabelled HAC1:
0.05nM
0.25nM
0.5nM
1nM
1.5 nM
0 5 10 15
0 5 10 15
0 5 10 15
0 5 10 15
0 5 10 15min
+cold HAC1
Radiolabelled HAC1:
0.05nM
0.25nM
0.5nM
1nM
1.5 nM
0 5 10 15
0 5 10 15
0 5 10 15
0 5 10 15
0 5 10 15min
+cold INSULIN
Radiolabelled HAC1:
0.05nM
0.25nM
0.5nM
1nM
1.5 nM
0 5 10 15
0 5 10 15
0 5 10 15
0 5 10 15
0 5 10 15min

Figure S3

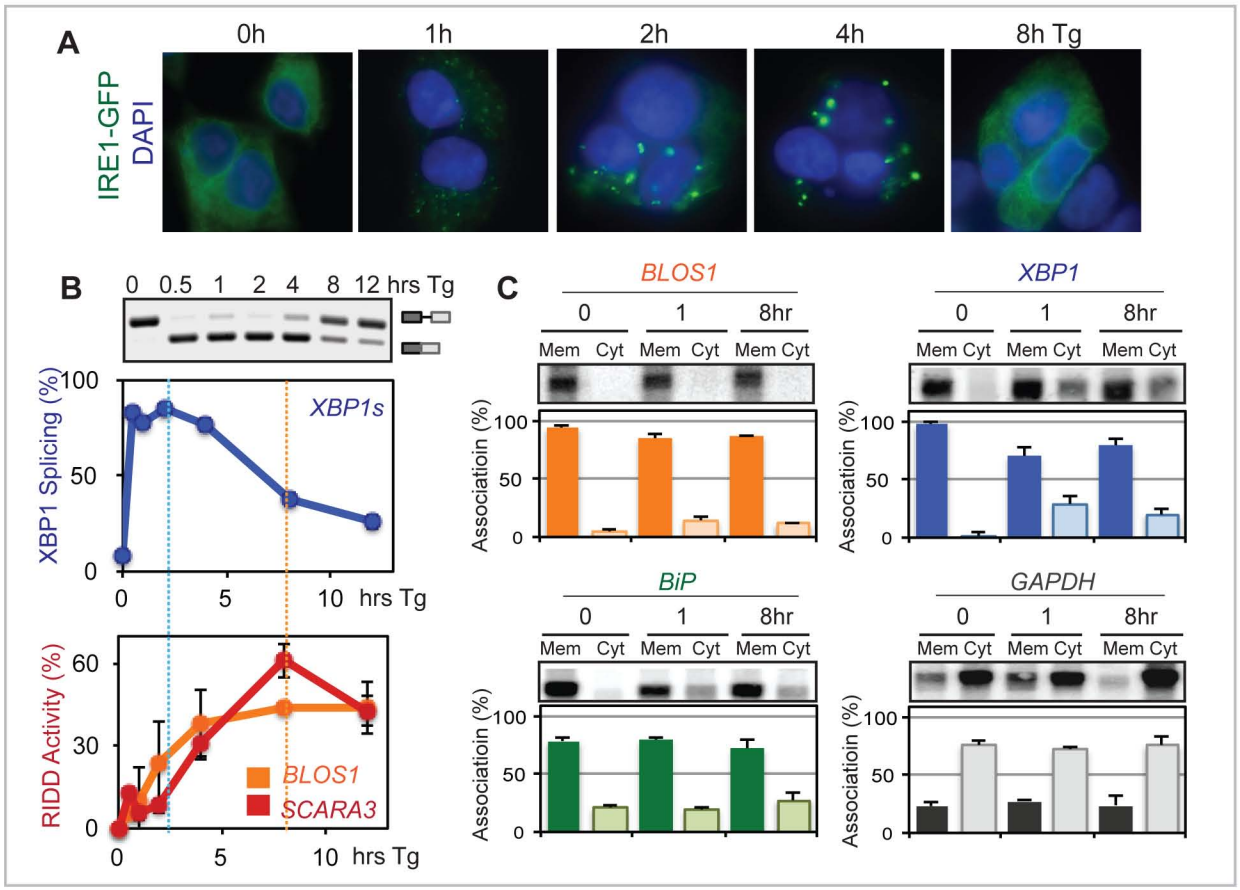
A
0h
1h
2h
4h
8h Tg
IRE1-GFP
DAPI
B
0 0.5 1 2 4 8 12 hrs Tg
XBP1 Splicing (%)
XBP1s
hrs Tg
RIDD Activity (%)
BLOS1
SCARA3
C
BLOS1
XBP1
BiP
GAPDH
0
1
8hr
Mem Cyt
Association (%)

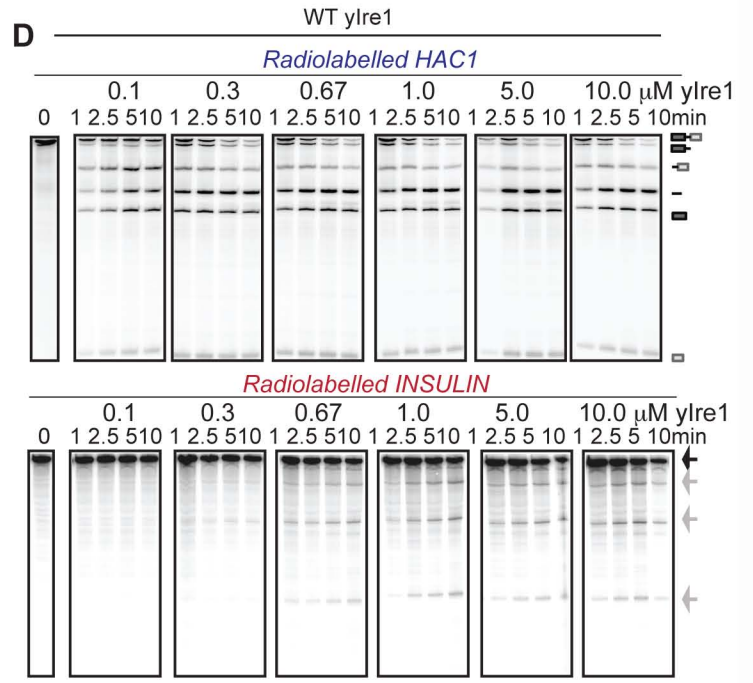
D
WT yIre1
Radiolabelled HAC1
0.1 0.3 0.67 1.0 5.0 10.0 μM yIre1
0 1 2.5 5 10 1 2.5 5 10 1 2.5 5 10 1 2.5 5 10 1 2.5 5 10 1 2.5 5 10min
Radiolabelled INSULIN

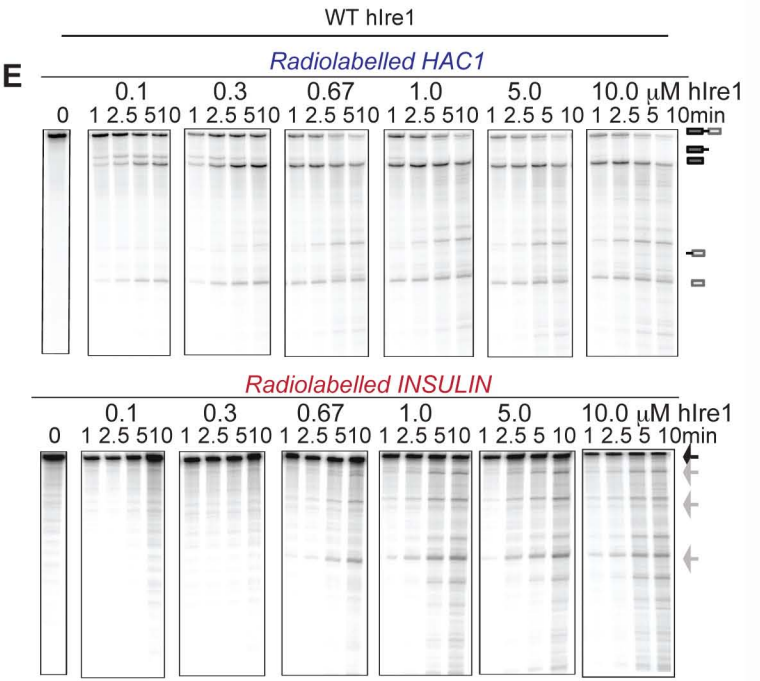
WT hIre1
E
Radiolabelled HAC1
0.1 0.3 0.67 1.0 5.0 10.0 μM hIre1
0 1 2.5 5 10 1 2.5 5 10 1 2.5 5 10 1 2.5 5 10 1 2.5 5 10 1 2.5 5 10min
Radiolabelled INSULIN

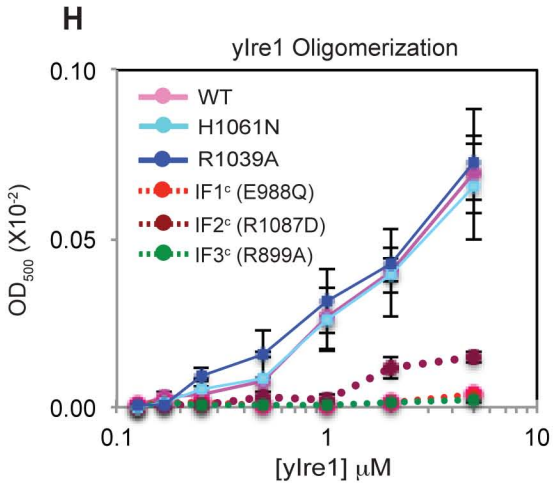
H
yIre1 Oligomerization
WT
H1061N
R1039A
IF1ᶜ (E988Q)
IF2ᶜ (R1087D)
IF3ᶜ (R899A)
OD500 (X10-2)
[yIre1] μM

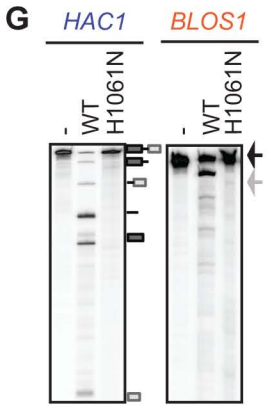
G
HAC1
BLOS1
-
WT
H1061N

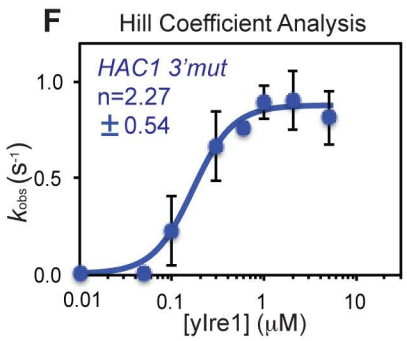
F
Hill Coefficient Analysis
HAC1 3'mut
n=2.27
±0.54
kobs (s-1)
[yIre1] (μM)

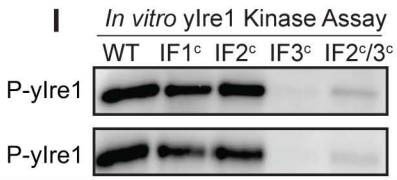
I
In vitro yIre1 Kinase Assay
WT IF1ᶜ IF2ᶜ IF3ᶜ IF2ᶜ/3ᶜ
P-yIre1
P-yIre1

Figure S4

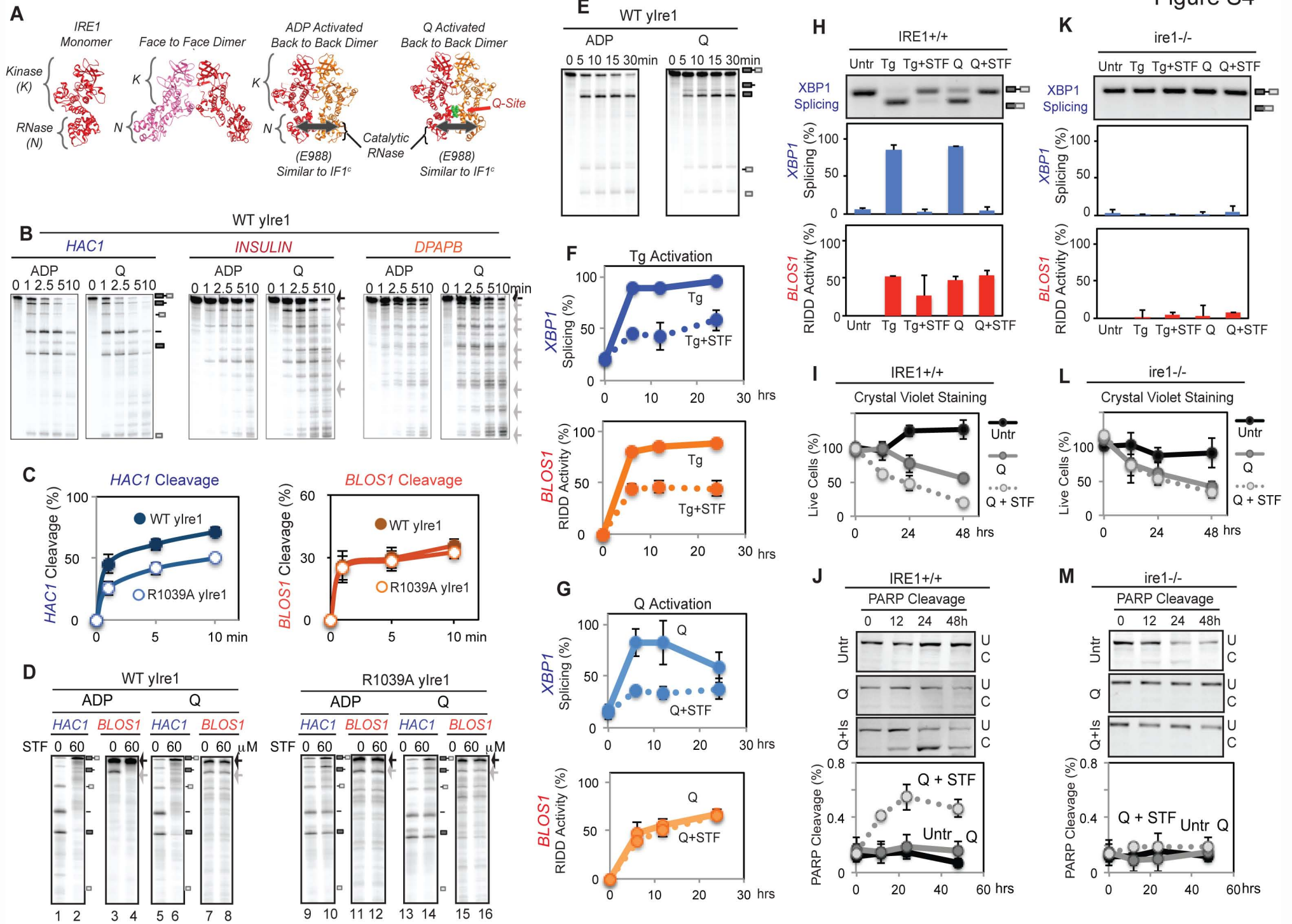
A
IRE1 Monomer
Face to Face Dimer
ADP Activated Back to Back Dimer
Q Activated Back to Back Dimer
Kinase (K)
RNase (N)
K
N
Q-Site
Catalytic RNase
(E988) Similar to IF1c
B
WT yIre1
HAC1
INSULIN
DPAPB
ADP
Q
0 1 2.5 5 10
min
C
HAC1 Cleavage
BLOS1 Cleavage
HAC1 Cleavage (%)
BLOS1 Cleavage (%)
WT yIre1
R1039A yIre1
min
D
WT yIre1
R1039A yIre1
ADP
Q
HAC1
BLOS1
STF 0 60 μM
1 2 3 4 5 6 7 8 9 10 11 12 13 14 15 16
E
WT yIre1
ADP
Q
0 5 10 15 30min
F
Tg Activation
XBP1 Splicing (%)
BLOS1 RIDD Activity (%)
Tg
Tg+STF
hrs
G
Q Activation
Q
Q+STF
hrs
H
IRE1+/+
Untr Tg Tg+STF Q Q+STF
XBP1 Splicing
XBP1 Splicing (%)
BLOS1 RIDD Activity (%)
K
ire1-/-
I
IRE1+/+
Crystal Violet Staining
Live Cells (%)
Untr
Q
Q + STF
hrs
L
ire1-/-
J
IRE1+/+
PARP Cleavage
0 12 24 48h
Untr
Q
Q+Is
U
C
PARP Cleavage (%)
Q + STF
Untr Q
hrs
M
ire1-/-

SUPPLEMENTAL FIGURE LEGENDS

Figure *S1*. Yeast Ire1 performs RIDD both *in vivo* and *in vitro*

(Related to Figure 1)

(A) RIDD in yeast (*S. cerevisiae*) during ER stress. WT (closed circle), *ire1Δ* (open circle), or *hac1Δ* (grey circle) cells were treated with tunicamycin (Tm) for up to 6 hrs and RNA was collected. RNA levels of *DAP2* and *MFα1* were determined by reverse transcription-followed by quantitative PCR (RT-qPCR). RNA decreased during ER stress only in WT and *hac1Δ* cells and not in *ire1Δ*, indicating RIDD where the decrease in RNA is IRE1 dependent, but HAC1 independent. Error bars shown in Figure *S1* all represent data from at least three independent repeats.

(B) *HAC1* Splicing in wild type IRE1 and *ire1Δ* strains during ER stress. The same RNA isolated from (A) was analyzed for *HAC1* splicing by Northern Blot. Un-spliced (top band) and spliced (bottom band) are indicated. *HAC1* splicing occurred only in WT cells and not in *ire1Δ* cells. *hac1Δ* cells did not show any *HAC1* signal by Northern Blot as anticipated (data not shown).

(C) *In vitro* cleavage of *HAC1/XBP1* by purified recombinant WT yeast IRE1 (yIre1) or human IRE1 (hIre1) as indicated. *In vitro* transcribed radiolabeled *HAC1*, *XBP1, or ACT1* RNA was incubated with 1μM WT yIre1 or WT hIre1 for up to 30 min upon addition of 2mM ADP. Cleavage fragments were analyzed by separation on a denaturing Urea 6% polyacrylamide gel. *HAC1* and *XBP1* RNA were cleaved by yIre1 and hIre1, respectively, whereas *ACTIN* RNA was cleaved by neither yIre1 nor hIre1.

(D) WT yIre1 cleaved *DAP2* or MFα1 RNA *in vitro*. Nuclease assays were performed using 1μM WT yIre1 and *in vitro* transcribed *DAP2* or MFα1 radiolabeled RNA. Cleavage fragments were analyzed upon incubation with ADP for indicated length of time. Uncut precursor is shown as black arrows and cleavage fragments are indicated with gray arrows.

(E) The invariant '**G**' residue critical for IRE1 cleavage present in *XBP1* mRNA 5' and 3' splice sites (5'SS and 3'SS) (Sidrauski and Walter, 1997) and in WT *INSULIN* RNA (Han et al., 2009) is mutated to "C" in mutant *INSULIN* RNA (mut *INSULIN*) (top panel). Incubation of mut *INSULIN* with WT yIre1 and 2mM ADP for 10 min diminished the cleavage at this site, but instead activated alternative cleavage sites.

(F) Activation Profile of yIre1 *in vitro*. To determine single turnover reaction conditions, *HAC1* RNA cleavage reactions were performed with the increasing concentrations of yIre1 ranging from 0.1-5 μM until there was no further increase in *HAC1* RNA cleavage activity. k_{obs} (s^{-1}) for *HAC1* RNA cleavage reaction at different concentration of yIre1 was calculated from profiles of % cleavage of *HAC1* RNA throughout time courses performed at different concentrations of yIre1. k_{obs} (s^{-1}) stayed at similar values when concentration of yIre1 became higher than 1μM and thus, we chose 3μM Ire1 for the subsequent competition experiments as a single turnover condition.

(G-H) Competition assays described in Figure 1C-1E. Reactions were performed with radiolabeled *HAC1* and 3μM yIre1 with increasing amounts of either cold (unlabeled) *HAC1* or cold *INSULIN* RNA (G) or cold *XBP1* RNA (H), as indicated.

(I-J) *XBP1* RNA cleavage by hIre1 was effectively competed by *HAC1* RNA but not *INSULIN* (RIDD) RNA. Competition assays were performed with radiolabeled *XBP1* RNA and 3μM yIre1 with 15 μM of either cold *HAC1* or cold *INSULIN* RNA. k_{obs} was calculated from reactions shown in I (J).

(K-L) Competition assays described in Figure 1F. Reactions were performed with radiolabeled *INSULIN* (K) or *BLOS1* (L) and 3μM yIre1 with increasing amounts of either cold *HAC1* or cold *INSULIN* RNA, as indicated.

Figure *S2*. Competition Assays of RIDD at Single Turnover and Steady State Conditions
(Related to Figures 1 and 2)

(A) Activity profile for RIDD. Similarly to Figure *S1F*, *INSULIN* RNA cleavage were performed with increasing concentration of yIre1 ranging from 0.1-15 μM using 0.25nM radiolabeled *INSULIN*. At 10μM of yIre1, there was no further increase in k_{obs} (s^{-1}) for *INSULIN* RNA cleavage activity. At 15μM of yIre1, competition experiments of radiolabeled *INSULIN* RNA were repeated with either cold *HAC1* or *INSULIN* RNA (Figure 1G).

(B) *INSULIN* RNA cleavage (RIDD substrate cleavage) by yIre1 was competed by cold *INSULIN* RNA but not by cold *HAC1* RNA using 15μM yIre1 cleaving 0.25nM radiolabeled *INSULIN* RNA. Competition experiments were performed with 0, 7.5, 15 or 50μM cold *HAC1* or *INSULIN* RNA. k_{obs} for these reactions are graphed in Figure 1G.

(C-D) Steady state competition experiments of radiolabeled *HAC1* RNA cleavage. To achieve steady state conditions, lower concentration of yIre1 (0.1 μM) was incubated with varying concentrations of either cold *HAC1* (C) or cold *INSULIN* (D) RNA competitors at 0, 0.15, 0.3, or 1.5μM and incubated with 2mM ADP for up to 15 min. % *HAC1* cleaved was calculated and graphed. Addition of 0.15, 0.3 or 1.5μM cold *HAC1* competitor resulted in a decrease in activity, while addition of 0.3 or 1.5μM cold *INSULIN* competitor also resulted in decreased activity.

(E) Non-competitive inhibition of *HAC1* RNA cleavage by RIDD RNA. Using steady state conditions described in (C) and (D), increasing concentrations of radiolabeled *HAC1* (ranging from 0.05-1.5nM) were incubated with 0.1μM yIre1 in the presence of no competitor, 1.5μM cold *HAC1* or cold *INSULIN* RNA. Results are shown as a Lineweaver-Burk plot and described in Figures 2A and 2B.

Figure *S3*. RIDD cleavage does not require IRE1 oligomerization
(Related to Figure 3)

(A) Formation of hIRE1 foci correlate with *XBP1* mRNA splicing but not with RIDD. HEK293 cells stably expressed hIRE1-GFP (Li et al., 2010) were treated with 200nM thapsigargin (Tg) for up to 8 hrs and visualized for IRE1 (green). Human IRE1 formed visible foci at 1, 2 and 4 hr time points, but dispersed by 8 hr. DAPI staining (blue) shows nucleus.

(B) Kinetics of *XBP1* mRNA splicing and RIDD activity in HEK293 cells when treated with Tg (200nM). Cells were collected at the indicated times and RNA was examined by reverse transcription (RT)-PCR to determine the percentage of spliced *XBP1* mRNA by gel-electrophoresis with un-spliced and spliced *XBP1* indicated (top panel). *XBP1* splicing was calculated by (spliced *XBP1*/(spliced + unspliced *XBP1* mRNA) X100%. The same cDNA was used to perform quantitative PCR (qPCR) using primers complimentary to *BLOS1* (orange) and *SCARA3* (dark red) mRNA, another RIDD target (Hollien et al., 2009). RIDD activity was calculated using [(*RIDD* mRNA in untreated cells - *RIDD* in treated cells) / *RIDD* in untreated cells] X100%. Blue line indicates high *XBP1* splicing activity at 2 hrs, while the orange & dark red lines indicate the peak of RIDD activity at 8 hrs. Error bars were generated from at least three independent experiments. It should be noted that *XBP1* mRNA splicing activity includes both IRE1 cleavage of the *XBP1* intron and the exon ligation steps, while RIDD activity includes degradation of IRE1 cleaved RNA fragments. Thus, the apparent kinetic relationships of *XBP1* mRNA splicing and RIDD may over-estimate kinetic differences of IRE1-dependent steps alone in HEK293 cells. This may also contribute differential kinetic relationships of *XBP1/HAC1* and RIDD substrate RNA cleavage observed

in vivo vs *in vitro* where both cleavage reactions occurred with similar kinetics (Figures 1A, S1C, S1D). Alternatively, an additional factor(s) may exist to modulate IRE1 cleavage of either *HAC/XBP1* or RIDD substrate RNA *in vivo*.

(C) Localization of IRE1 RNA substrates. Both *XBP1* and RIDD substrate RNA were associated with ER membrane prior to ER stress induction. HEK293 cells were treated with 200nM Tg for up to 8hrs, and cytosol (Cyt) and ER membrane (Mem) fractions were separated using serial detergent extractions as described in (Stephens et al., 2005). RNAs isolated from these fractions were analyzed by Northern blots probing *BLOS1*, *XBP1,* and *KAR2/BIP* mRNA. Most of both *XBP1* and *BLOS1* RNA were localized to the ER membrane even prior to UPR induction (compare RNA in the untreated (0) vs Tg treated cells for 1 or 8 hrs). As reported previously, splicing released *XBP1* mRNA into the soluble cytoplasmic fraction (Stephens et al., 2005). In contrast, the majority of *GAPDH* mRNA was localized to the cytosolic fraction. Consistent with previous reports, some GAPDH was found in the membrane fraction (Stephens et al., 2005). Standard deviations were calculated from at least three independent experiments.

(D-E) To determine Hill Coefficients, increasing amounts of either yIre1 (D) or hIre1 (E) were used to perform nuclease reactions (Korennykh et al., 2009). Un-cleaved and cleaved fragments of RNA were indicated. k_{obs} (s^{-1}) were graphed in Figures 3A.

(F) Hill coefficient analysis for *HAC1* with the 3' stem loop mutated (*HAC1 3'* mutant). The 3' stem loop mutation has been shown to block cleavage by IRE1 (Sidrauski and Walter, 1997). Nuclease reactions described in (D) were done using *HAC1* 3' mutant. Hill Coefficients for *HAC1* 3' mutant (2.27±0.54) is similar to unmodified WT *HAC1* (2.13±0.38), indicating that both are cooperative and that numbers of the cleavage sites do not affect the Hill Coefficients.

(G) H1061N yIre1 is nuclease dead for both *HAC1* RNA cleavage and RIDD. Either WT yIre1 or H1061N yIre1 was activated with 2mM ADP for 15 min allowing the cleavage of either *HAC1* or *BLOS1* RNA.

(H) Oligomerization assays as described in (Korennykh et al., 2009) was performed on either WT yIre1, H1061N or R1039A mutants, or interface mutants $IF1^c$, $IF2^c$, and $IF3^c$. At increasing concentrations, WT yIre1, H1061N yIre1 and R1039A yIre1 showed significant increases in OD_{500}, while OD_{500} for $IF1^c$, $IF2^c$ and $IF3^c$ yIre1 mutants did not show such increase. WT yIre1 (solid pink), H1061N yIre1 (solid light blue), R1039A yIre1 (solid dark blue), $IF1^c$ mutant E988Q yIre1 (dotted red), $IF2^c$ mutant R1087D yIre1 (dotted maroon), $IF3^c$ mutant R899A yIre1 (dotted green) are shown.

(I) *In vitro* kinase assay for Ire1 oligomerization mutants. WT and interface mutants $IF1^c$ (E988Q), $IF2^c$(R1087D), $IF3^c$ (R899A), or a $IF2^c/IF3^c$ double interface mutant were tested for their abilities to undergo autophosphorylation in *in vitro. In vitro* kinase reactions were performed upon incubation with γ^{32}P-ATP, and analyzed by SDD-PAGE, followed by autoradiography.

Figure S4. RIDD activation leads to apoptosis

(Related to Figure 4)

(A) Back to back dimer of IRE1 forms a catalytically active RNase site (Ali et al., 2011; Lee et al., 2008; Wiseman et al., 2010). An IRE1 monomer (red) containing the kinase and RNase domains is shown (Left). To initiate trans-autophosphorylation, two IRE1 monomers adopt a face to face conformation where the nucleotide binding pockets of each monomer can access the activation loop of the other (Ali et al., 2011). In the face-to-face dimer, the catalytic RNase sites are inactive and pointing away from each other, and face to face interactions were not present in the crystalized oligomer (Figure 3C). Formation of a back to back dimer where the nucleotide binding pockets are facing away from each other juxtaposes the RNase domains and forms an active nuclease site. Formation of the back-to-back dimer can be formed with ADP binding to the nucleotide pocket and with quercetin in the Q-site. The back-to-back dimer forms the building block of the IRE1 oligomer (Figure 3C) and the interface $IF1^c$ is indicated.

(B) Quercetin (Q) activation of RIDD. Incubation of yIre1 with Q (100μM) induced cleavage of *HAC1* RNA at kinetics and the extent similar to that by ADP. Q also induced Ire1 to cleave *INSULIN* or *DAP2* RIDD substrates efficiently *in vitro*. Precursor mRNA and cleavage products were indicated as previous figures. IRE1 dependent cleavage reactions of both *HAC1* and RIDD substrate RNA are faster with Q than ADP. This may be due to the ability of Q to form the back-to-back IRE1 dimer dimers (Figure S4A) (Wiseman et al., 2010), which would be a building unit for the fully active oligomerized IRE1. Though no cooporativity between IRE1 is involved (Figure 3A), the back-to-back dimer formation may help to stabilize a specific conformation of IRE1 needed for RIDD substrate cleavage.

(C) R1039A yIre1 was reduced for *HAC1* cleavage, but retained RIDD cleavage. 1μM of either WT yIre1 (closed circle) or R1039A yIre1 (open circle) was incubated with 2mM ADP for up to 10 min. An amino acid change at R1039 to Alanine decreased the ability of yIre1 to cleave *HAC1* RNA (left panel). On the other hand, it did not

show the significant change in *BLOS1* RNA (right panel) where both WT and R1039A yIre1 showed the same *BLOS1* RNA cleavage activity. Error bars represent data from at least three independent experiments.

(D) Representative RNase reactions for Figures 4D and 4E. WT yIre1 (1μM) was incubated with either ADP or Q for 30 min to cleave *HAC1* or *BLOS1* RNA, in the presence or absence of STF-083010 (Papandreou et al., 2011). *HAC1* RNA cleavage was effectively inhibited when 60μM STF-083010 (STF) was added (lanes 1&5 (no inhibition) vs 2&6 (with STF)). In contrast, *BLOS1* RNA cleavage was inhibited by STF when ADP was used as a cofactor (lane 4), but not inhibited when Q was added as a co-factor (lane 8). Additionally, similar experiments were performed with R1039A yIre1 (lanes 9-16). STF did not inhibit either *HAC1* or *BLOS1* RNA cleavage reactions.

(E) Quercetin (Q) activates hIre1 in *in vitro*. hIre1 was activated with either 2mM ADP or 100μM Q and incubated with radiolabeled *XBP1* in an *in vitro* nuclease reaction for the indicated length of time. Addition of Q alone activated hIre1 cleavage of *XBP1* RNA to a similar extent as ADP.

(F-G) Q activated RIDD is not inhibited by STF in wild type MEFs. Wild type MEFs were treated with 200nM thapsigargin (Tg) or Tg + 60μM STF (F), for up to 24 hrs. mRNA was isolated and levels of the spliced *XBP1* mRNA or *BLOS1* mRNA were determined by performing RT-PCR or RT-qPCR, respectively. STF inhibited *XBP1* mRNA splicing and cleavage of *BLOS1* RNA induced upon Tg treatment of cells. Similarly, wild type MEFs incubated with Q (450μM) (G) were also activated for *XBP1* splicing and RIDD. In this case, however, STF was unable to inhibit *BLOS1* RNA cleavage while *XBP1* splicing was effectively inhibited. Error bars represent at least three independent experiments. RIDD activity (%) was calculated as described before (Figure S3B).

(H)(K) STF inhibits *XBP1* mRNA splicing, but does not impact RIDD for Q-activated IRE1 *in vivo*. Mouse embryonic fibroblasts (MEFs) carrying WT mouse IRE1 (H) or *ire1* knockout (K) were incubated with Tg, Tg+STF , Q (450μM), and Q+STF or untreated for 2 hrs. RNA isolated from each reaction were analyzed by RT-qPCR for both *XBP1* splicing (H or K, top panel) and RIDD activity. Positions of spliced and un-spliced *XBP1* RNA were indicated. Quantitation of spliced *XBP1* RNA and *BLOS1* mRNA cleavage was shown.

(I)(L) WT IRE1 (I) or *ire1* knockout (L) MEFs were incubated with Q, Q+STF, or untreated for up to 48 hrs and stained with crystal violet. Numbers of cells stained with % of crystal violet (live cells) were calculated.

(J)(M) Upon treatment with Q, or Q+STF, or untreated WT-IRE1 cells (J) or *ire1* knockout MEFs (M) for indicated length of time, total cell extracts were prepared and examined for apoptosis by examining PARP cleavage upon performing western blots using anti-PARP antibody. Positions of uncleaved (U) and cleaved (C) PARP are indicated and quantitated to calculate % cleavage of PARP at each time point (bottom panel). Error bars represent at least three independent experiments.

SUPPLEMENTAL EXPERIMENTAL PROCEDURES

In Vitro IRE1 Substrates: HAC1, XBP1, and RIDD

HAC1 substrate (508 nt) used in all the *in vitro* RNase reactions was *in vitro* transcribed from a plasmid described previously (pCF187) (Sidrauski and Walter, 1997). Human *XBP1* substrate (444 nt) (Lee et al., 2002) was made by PCR amplifying human cDNA with primers containing a T7 site (F)-TAATACGACTCACTATAGGGAGAAGAACCAGGAGTTAAGAC; (R)-TAAGACTAGGGGCTTGGTATATATGTG. RIDD substrates were also prepared by PCR amplifying cDNA from the appropriate organism with primers containing a T7 site. *INSULIN* (mouse INSULIN-2) RNA (503 nt) was prepared as described (Han et al., 2009). *BLOS1* (mouse *BLOS1*) (379 nt) and yeast *DPAPB* (DAP2) (538 nt) substrate RNA was prepared from a DNA fragment prepared by PCR amplification using mouse or yeast cDNA, respectively, using the following primers: *BLOS1*: (F) ATGGTACCTAATACGACTCACTATAGGATGCTGTCCCGCCTGC, (R) ATGAGCTCCTAGGATGGTGCAGACTGCAG; *DAP2*: (F) ATGGTACCTAATACGACTCACTATAGGGCAGAAAAATGCGACAAAGG; (R) ATGAGCTCTTGAAATGTCTTCCGCCATC. PCR products were then phenol/chloroform extracted and ethanol precipitated and used as templates for *in vitro* transcription

In Vitro Transcription of RNA Substrates

In vitro transcription of radiolabeled RNA substrates has been described previously (Chawla et al., 2011; Sidrauski and Walter, 1997). Briefly, *in vitro* transcription was performed using T7 RNA polymerase (Promega) at 37 °C, 1mM each of ATP, CTP, GTP, 100μM of UTP, and 50 μCi of α^{32}P-UTP (3000Ci/mmol), and 1 μg of template DNA. Transcripts were separated on a 6% UREA-PAGE gel and radiolabeled RNA products were gel extracted by phenol/chloroform followed by ethanol precipitation. Activity of probes was measured by scintillation counter, and diluted to an activity of 20,000 cpm/μl, and based on the efficiency of the scintillation counter, this was equivalent to 10 fmol/μl of radiolabeled RNA.

Unlabeled (cold) RNA was transcribed using MEGAscript T7 Kit (Life Technologies) according to manufacturer's instructions, using 1μg of template DNA. To ensure that the cold RNA was equivalent to the radiolabeled RNA, cold RNA was gel purified side by side with its radiolabeled counterpart. Concentration was then determined upon quantitation by NanoDrop (Thermo).

Protein Purification and Site Directed Mutagenesis

For this study, we used a 6XHis-tagged WT yIre1 containing the entire cytosolic domain (642aa-1115aa) integrated into an expression vector (pET15b). Proteins were expressed in *E. coli* and purified using a Ni-NTA

column (Invitrogen) as described (Sidrauski and Walter, 1997). Recombinant human IRE1α (hIre1) was expressed and purified using a Baculovirus SF-9 expression system and purified using a Ni-NTA column, as previously described (Niwa et al., 1999). Point mutations in yIre1 were generated using QuickChange Site Directed Mutagenesis (Stratagene/Agilent) according to manufacturer's instructions using the plasmid containing WT yIre1 (642-1115), and point mutations were confirmed by sequencing.

In vitro Nuclease Assay and Kinetic Analysis

In vitro nuclease assays were performed as described in (Sidrauski and Walter, 1997). Reactions were performed in a 20 µl volume in nuclease reaction buffer (40mM Hepes, 7.0, 10mM $Mg(OAc)_2$, 50mM KOAc, 5mM DTT) at 30°C for the indicated amount of time, unless otherwise indicated. Standard nuclease reactions contained 2mM ADP, 100µM quercetin (Sigma) or 60µM STF-083010 (Papandreou et al., 2011) when indicated, 1µM either yIre1 or hIre1, and 0.5nM radiolabeled RNA. For reactions with L745G yIre1, 20µM 1NM-PP1 (Calbiochem) was used. Reactions were started when radiolabeled substrate was added, and reactions were stopped by addition of stop buffer (7M Urea, 350mM NaCl, 10mM Tris pH 7.6, 10mM EDTA, 1% SDS) and RNA was extracted using phenol/chloroform, ethanol precipitated, and analyzed on a denaturing 6% Urea acrylamide gel. To determine reaction rates, signal from each lane was quantified using Typhoon 9400 (GE Healthcare) and analyzed using ImageQuant (GE Healthcare). Based on the numbers of the U residues in individual cleaved fragments, we calculated the molar concentration of each cleavage products. % cleavage for *HAC1, XBP1* or RIDD RNA was calculated as [(sum of cleaved RNA fragments) / (uncleaved RNA + sum of cleaved RNA fragments)] X100%. For each time course, an activation curve was generated by plotting time (x) vs. cleaved substrate (y). Using this data, non-linear regression analysis was performed in SigmaPlot (Systat Software, Inc) to generate a curve using the exponential curves function. k_{obs} was generated using the initial slope of the generated curve obtained in SigmaPlot.

Determination of Hill Coefficients

Hill Coefficients were determined as previously described in (Korennykh et al., 2009). Briefly, standard nuclease assays were set up with nuclease buffer, 2mM ADP, and varying concentrations of either yIre1 or hIre1, as described. Reactions were performed in 20µl, and started when 0.5nM radiolabeled RNA (either *HAC1, INSULIN, HAC1 3' mut* for yIre1 or *XBP1, INSULIN* for hIre1) was added. Reactions were stopped with stop buffer and analyzed on 6% UREA gel, and molar values for uncleaved and cleaved products were calculated. For each concentration of Ire1, k_{obs} was calculated as described above and values were plotted ([Ire1] vs k_{obs}) and fitted using GraphPad Prism 5 (La Jolla, CA). The Hill coefficient was calculated by Prism using a four parameter logistic equation under the sigmoidal dose response curve with variable slope function. We interpret a

non-cooperative Hill coefficient of 1 as IRE1 acting within a dimer since monomeric IRE1 is inactive (Lee et al., 2008). Experiments were done at least three times with standard deviations shown.

Structural Analysis of IRE1

Structural analysis was done using Chimera (http://www.cgl.ucsf.edu/chimera) (Pettersen et al., 2004) and structure prediction was done using Phyre2 (*www.sbg.bio.ic.ac.uk/**phyre2**/) (Kelley and Sternberg, 2009). Structures used were: 3FBV* (Korennykh et al., 2009) *for yIre1 oligomers (Figure 3C), 3P23* (Ali et al., 2011) *for hIre1 face to face dimer (Figure S4A), 2RIO* (Lee et al., 2008) for ADP activated yIre back to back dimer (Figure S4A), *and 3LJO* (Wiseman et al., 2010) *for quercetin activated yIre1 back to back dimer (Figure S4A).*

Cell Culture and IRE1 Foci Microscopy

HEK 293 cells stably transfected with IRE1-GFP (Li et al., 2010) were grown in DMEM media (Cellgro) with 10% FBS and 100 U/ml penicillin, and 100μg/ml streptomycin (Mediatech) in 5% CO_2 at 37°C. To visualize IRE1 foci, cells were grown on a cover slip and the expression of IRE1-GFP was induced upon incubation with 10nM Doxycycline for 24 hrs before start of Thapsigargin (Tg) treatments. Cells were treated with 200nM Tg for up to 8 hrs. Cover slips were then washed with PBS and fixed with 4% PFA. For visualization of IRE1-GFP, cells were then mounted with mounting media containing 1μg/mL DAPI (Pierce) and visualized in the green channel by microscope (Axiovert 200M; Carl Zeiss MicroImaging, Inc.) with a 100X 1.3 NA objective.

Yeast Culture and Northern Blots

Yeast strains used in this study were described in (Chawla et al., 2011); WT (MNY1000), *ire1Δ* (MNY1655), *hac1Δ* (MNY1662). Yeast strains were grown in YPD medium (1% yeast extract, 2% bactopeptone, and 2% glucose) at 30 °C to an OD_{600} of ~0.5 before Tunicamycin (Tm) to a final concentration of 1μg/ml was added and incubated for indicated length of time. At each time point, cells were collected and RNA was isolated for Northern Blot analyses as described previously (Chawla et al., 2011). Briefly, RNA was extracted using the hot phenol method, and RNA was separated on 1.5% agarose gels containing 6.7% formaldehyde and transferred to a Duralon-UV membrane (Agilent Technologies). Splicing of *HAC1* mRNA was examined by hybridization of the membrane with radiolabeled HAC1 probe at 65 °C overnight, and exposed via phosphoimager screen (GE Healthcare). Quantitation was performed using a Typhoon Imager system (GE Healthcare).

Kinase Assay

In vitro Kinase assays were performed as described (Chawla et al., 2011). WT yIre1 or mutant yIre1 proteins were incubated in kinase buffer (10mM Hepes pH 7.5, 5mM $Mg(OAc)_2$, 25mM KOAc, 1mM DTT) with 200 μM of unlabeled ATP and 167 μCi of ^{32}Pγ-ATP (7000Ci/mmol) in a volume of 20μl. Reactions were incubated at 30

°C for 30 min, and hot SDS Loading Buffer and incubation at 95 °C was used to stop the reaction. Samples were immediately run on a 7% SDS-PAGE gel. Phosphorylation was determined by autoradiography and scanned on a Typhoon 9400 (GE Healthcare).

Fractionation of ER

Cells were treated for up to 8 hrs as indicated, washed twice with PBS, and re-suspended in Fractionation Buffer: 10mMHEPES [pH 7.4], 1mM EDTA, 0.25Msucrose, protease inhibitors (Leupeptin, Pepstatin, Aprotinin). Cells were then homogenized by passage through a 27 gage needle and centrifuged at 500Xg for 3min at 4 °C. 150µl of supernatant was then mixed with 2.5M sucrose in Fractionation Buffer, and a flotation gradient was assembled with 1.8M, 1.3M, 0.8M sucrose fractions, with the 1.3M fraction containing the rough microsomes. The gradient was centrifuged at 100,000Xg for 12 hrs, and the 1.3M and 2.5M solutions, corresponding to the ER and cytosolic portions, respectively, were collected. RNA was then extracted using Trizol (Invitrogen) and 10µg of RNA of each fraction was used for Northern Blots as described above.

Oligomerization Assay

Oligomerization assay was done as previously reported (Korennykh et al., 2011). Briefly, reactions were set up using nuclease reaction buffer (40mM Hepes, 7.0, 10mM $Mg(OAc)_2$, 50mM KOAc, 5mM DTT), the indicated amount of WT or mutant yIre1, and 2mM ADP. All reactions were performed in 20µl and incubated for 15 min at 30 °C to allow for oligomerization. The optical density of the sample was measured at 500 nm using a UV-visible spectrophotometer (NanoDrop 2000, Thermo Scientific). Readings were blanked using a reaction without yIre1.

Cell Culture and Determination of XBP1 Splicing and RIDD in vivo

All mammalian cells were cultured in DMEM media (Cellgro) with 10% FBS and 100 U/ml penicillin, and 100ug/ml streptomycin (Mediatech). Cells were grown in 5% CO_2 at 37°C and treated with 200nM Thapsigargin (Calbiochem), 450µM Quercetin (Sigma), or STF-083010 (60µM) (Papandreou et al., 2011) as indicated.

Determination of spliced *XBP1* was performed as described (Lin et al., 2007). Briefly, total RNA was prepared from cells using Trizol (Invitrogen), and 1µg of total RNA was reverse transcribed using Maxima Reverse Transcriptase (Fermentas) to obtain cDNA. cDNA was then PCR amplified using the primers for *XBP1*: 5'-TTACGGGAGAAAACTCACGGC-3' and 5'-GGGTCCAACTTGTCCAGAATGC-3', resulting in a 289 bp fragment corresponding to unspliced *XBP1*, and a 263 bp spliced *XBP1* fragment. Fragments were resolved on a 2.5% agarose gel, and quantified using a Typhoon 9400 fluorescent scanner (GE Healthcare). *XBP1* splicing % was calculated by: [(spliced *XBP1*/(spliced *XBP1*+ unspliced *XBP1*)]X100%.

Determination of RIDD was performed as described (Hollien et al., 2009). Briefly, the same cDNA from

XBP1 splicing assays was used to perform quantitative PCR (qPCR). Reactions were done in triplicate (5ng of input RNA per reaction) for each pair of primers using SYBR Green PCR Master Mix (Applied Biosystems) and 400nM of each primer in a 25μl reaction and analyzed on an ABI Prism 7200 Sequence Detector (Applied Biosystems). Samples were run and quantified using the Standard Curve Method, and expression of each gene was normalized to 18S ribosomal RNA which did not significantly change in any of the conditions. After each run, Melting Curve Analysis was performed to confirm amplification of a single product. Error bars represent standard deviations of the mean calculated from at least three independent experiments. RIDD Activity was calculated by: [(*RIDD* mRNA in untreated cells - *RIDD* in treated cells) / *RIDD* mRNA in untreated cells] X100%. The following primer sets were used for RIDD: *BLOS1* 5'-CAAGGAGCTGCAGGAGAAGA-3' 5'-GCCTGGTTGAAGTTCTCCAC-3'; *SCARA3* 5'-TGCATGGATACTGACCCTGA-3' 5'-GCCGTGTTACCAGCTTCTTC-3' *DAP2*: 5'-GGCTGCGTGGTGGTCAC-3' 5'-CGCATTTCGGGGTATATATCC-3'; *MFα1*: 5'-CGGCTGAAGCTGTCATCG-3'5'-GATACCCCTTCTTCTTTAGCAGCA-3'.

Apoptosis Assays – PARP and Crystal Violet Staining

Construction of cells stably expressing human-yeast chimeric IRE (hyIRE1) containing 1-549aa of hIRE1 and 658-1115aa of yIRE1 was done as described previously (Wiseman et al., 2010). Ire1 knockout MEFs were stably transduced with either hyIRE1 or empty vector and treated with either 200nM thapsigargin (Calbiochem), 450μM Quercetin as described (Wiseman et al., 2010), or 60μM STF-083010 as indicated for up to 48 hrs. RNA was extracted and cDNA was prepared to perform *XBP1* splicing and RIDD activity assays as described above.

Crystal Violet Staining assays were performed in 6 well plates with 2 $X10^5$ cells plated 24hrs before treatment. After treatment, cells were fixed with 10% Formaldehyde; 0.9% NaCl, and stained with Crystal Violet (10% EtOH, 0.05% NaCl, 0.35% Formaldehyde, 0.15% Crystal Violet in 1X PBS). Cells were carefully washed 5 times with 1X PBS, removing excess dye from the plates and leaving only the cells stained. Crystal violet from the cells was then extracted with 2ml 1% SDS in 1X PBS and read by spectrophotometer at an absorbance of 595nm to quantify. The amount of Live Cells (%) (in Figures 4G, S4I, & S4L) was calculated by [(Crystal Violet in untreated cells – Crystal Violet treated cells) / Crystal Violet in untreated cells]X100%.

For analyses of PARP cleavage, cells were collected at each time point and total cell extract was prepared using RIPA buffer (20 mM HEPES (pH 7.4), 150mM NaCl, 1mM EDTA, 1% NP-40, 0.25% NaDeoxycholate, 0.1% SDS, 10mM NaF, 1mM NaVO4, 1mM PMSF, 1mM PMSF, 100u/ml Aprotinin, 1.4 μg/ml Pepstatin, 1μg/ml Leupeptin). Total protein concentrations were normalized by BCA assay (Pierce) and separated on an 8% SDS-PAGE followed by performing western blots using anti-PARP antibody (Cell Signaling) to detect uncleaved PARP and cleaved fragments. PARP Cleavage (%) was calculated using [(cleaved PARP/(uncleaved PARP+ cleaved PARP)]X100%.

SUPPLEMENTAL REFERENCES:

Kelley, L.A., and Sternberg, M.J. (2009). Protein structure prediction on the Web: a case study using the Phyre server. Nature protocols *4*, 363-371.

Niwa, M., Sidrauski, C., Kaufman, R.J., and Walter, P. (1999). A role for presenilin-1 in nuclear accumulation of Ire1 fragments and induction of the mammalian unfolded protein response. Cell *99*, 691-702.

Pettersen, E.F., Goddard, T.D., Huang, C.C., Couch, G.S., Greenblatt, D.M., Meng, E.C., and Ferrin, T.E. (2004). UCSF Chimera--a visualization system for exploratory research and analysis. Journal of computational chemistry *25*, 1605-1612.

Stephens, S.B., Dodd, R.D., Brewer, J.W., Lager, P.J., Keene, J.D., and Nicchitta, C.V. (2005). Stable ribosome binding to the endoplasmic reticulum enables compartment-specific regulation of mRNA translation. Molecular biology of the cell *16*, 5819-5831.